Novel pathways in cholesterol metabolism to combat cardiometabolic diseases

Zhou, E.

Colesevelam enhances the beneficial effects of brown fat activation on hyperlipidemia and atherosclerosis development

Enchen Zhou*, Geerte Hoeke*,Zhuang Li, Arthur C. Eibergen, Amber W. Schonk, Martijn Koehorst, Renze Boverhof, Rick Havinga, Folkert Kuipers, Tamer Coskun, Mariëtte R. Boon, Albert K. Groen, Patrick C.N. Rensen, Jimmy F.P. Berbée, Yanan Wang
**Authors contributed equally*

Cardiovasc Res 2020 Aug 1; 116(10):1710-1720

Abstract

Background

Brown fat activation accelerates the uptake of cholesterol-enriched remnants by the liver and thereby lowers plasma cholesterol, consequently protecting against atherosclerosis development. Hepatic cholesterol is then converted into bile acids (BAs) that are secreted into the intestine and largely maintained within the enterohepatic circulation. We now aimed to evaluate the effects of prolonged brown fat activation combined with inhibition of intestinal BA reabsorption on plasma cholesterol metabolism and atherosclerosis development.

Methods and results

*APOE*3-Leiden.CETP* mice with humanized lipoprotein metabolism were treated for 9 weeks with the selective β3-adrenergic receptor (AR) agonist CL316,243 to substantially activate brown fat. Prolonged β3-AR agonism reduced fecal BA excretion (-31%), while markedly increasing plasma levels of total BAs (+258%), cholic acid-derived BAs (+295%) and chenodeoxycholic acid-derived BAs (+217%), and decreasing the expression of hepatic genes involved in BA production. In subsequent experiments mice were additionally treated with the BA sequestrant Colesevelam to inhibit BA reabsorption. Concomitant intestinal BA sequestration increased fecal BA excretion, normalized plasma BA levels and reduced hepatic cholesterol. Moreover, concomitant BA sequestration further reduced plasma total cholesterol (-49%) and non-high-density lipoprotein-cholesterol (-56%), tended to further attenuate atherosclerotic lesion area (-54%). Concomitant BA sequestration further increased the proportion of lesion-free valves (+34%) and decreased the relative macrophage area within the lesion (-26%) thereby further increasing the plaque stability index (+44%).

Conclusions

BA sequestration prevents the marked accumulation of plasma BAs as induced by prolonged brown fat activation thereby further improving cholesterol metabolism and reducing atherosclerosis development. These data suggest that combining brown fat activation with BA sequestration is a promising new therapeutic strategy to reduce hyperlipidemia and cardiovascular diseases.

Introduction

Atherosclerosis represents the most common cause of cardiovascular diseases. A prominent risk factor for atherosclerosis is hyperlipidemia, i.e. high levels of low-density lipoprotein cholesterol (LDL-C) and triglycerides (TG) in the circulation. Currently, reducing circulating atherogenic lipoproteins with lipid-lowering medication, such as statins and PCSK9 inhibitors, remains the major strategy to prevent acute cardiovascular events. However, only 30% of all cardiovascular events can be prevented by such treatment strategies [1], illustrating the need for new therapeutic strategies.

Brown fat is present in mammals as well as in (adult) humans and is an emerging target to combat hyperlipidemia and atherosclerosis [2-4]. Cold exposure, the best known physiological activator of brown fat, leads to the release of noradrenalin from sympathetic nerves that innervate brown fat. Noradrenalin binds to the β3-adrenergic receptor (β3-AR) on brown adipocytes, resulting in their activation to produce heat [5]. As the β3-AR is highly expressed on brown and white adipocytes, and white fat does not substantially contribute to energy expenditure, the cold-stimulated activation of brown fat inducing thermogenesis can be pharmacologically mimicked by selective β3-AR agonists such as CL316,243 compound, one of the most selective β3-AR agonists available [6]. Since heat generation is an energy consuming process, activated brown fat takes up large amounts of nutrients from the circulation, mainly TG-derived fatty acids (FAs) from TG-rich lipoproteins (TRLs; i.e., very-low-density lipoproteins (VLDL) and chylomicrons) [7, 8]. As a result, brown fat activation accelerates the formation and uptake of cholesterol-enriched lipoprotein remnants by the liver, thereby protecting from hyperlipidemia and atherosclerosis development [7]. In addition to reducing cholesterol-enriched TRL remnant levels, β3-AR agonism also improves high-density lipoprotein (HDL) functionality as reflected by increased reverse cholesterol transport (RCT) [7, 9]. Collectively, these studies show that β3-AR agonism increases cholesterol delivery towards the liver via both accelerating the clearance of cholesterol-enriched TRL remnants and improving HDL-mediated RCT.

Hepatic cholesterol turnover is mainly mediated by fecal excretion as bile acids (BAs) and, to a lesser extent, by fecal excretion of neutral sterols [10]. Hepatocytes synthesize primary BAs, i.e., cholic acid (CA) and chenodeoxycholic acid (CDCA), via the so-called classic pathway; while CDCA can also be synthesized via an alternative pathway [11]. In mice, but not in humans, CDCA can be converted into more hydrophilic species, the so-called muricholic acids (MCAs) [12]. Newly synthesized BAs are temporarily stored in the gallbladder and are secreted into the duodenum upon food ingestion to serve as detergents for absorption of nutrients [13]. By the enzymatic action of gut bacteria, part of the primary BAs are converted into secondary BAs. In the terminal ileum, 95% of BAs are reabsorbed by active transport with remaining BAs excreted in feces. Reabsorbed BAs mainly circulate back through the portal vein to the liver completing one cycle of enterohepatic circulation [14]. BA synthesis is regulated by enterohepatic circulation of BAs via farnesoid X receptor (FXR), which inhibits transcription of genes in BA synthesis [15]. The enterohepatic circulation can be interrupted by BA sequestrants, which increases clearance of plasma (V)LDL-C by promoting conversion of hepatic cholesterol into BAs and up-regulation of hepatic LDL receptors. In fact, BA sequestrants such as Cholestyramine and Colesevelam have been proven to be effective to treat dyslipidemia and prevent cardiovascular diseases [16].

Interestingly, both short-term and long-term activation of brown fat increases cholesterol delivery towards the liver [7, 17]. Moreover, we previously showed that long-term activation of brown fat significantly increased hepatic cholesterol accumulation [17]. Since BA synthesis is

the main pathway for hepatic cholesterol catabolism, short-term activation of brown fat indeed has been linked to increased BA production and increased fecal BA excretion [18]. However, how long-term brown fat activation influences BA metabolism and whether manipulation of BA metabolism on top of brown fat activation would lead to additional benefits on cholesterol metabolism and atherosclerosis development has not been studied yet. Thus, the aim of the current study was to evaluate the effects of prolonged brown fat activation via β3-AR agonism on cholesterol and BA metabolism. In addition, we assessed whether inhibiting intestinal BA reabsorption beneficially influences the effects of prolonged β3-AR agonism on cholesterol turnover and atherosclerosis development. To this end, we treated hyperlipidemic *APOE*3-Leiden(E3L).CETP* mice, a well-established model for human-like lipoprotein metabolism and atherosclerosis[19, 20], with or without the selective β3-AR agonist CL316,243 to activate brown fat for 9 weeks. In subsequent experiments, *E3L.CETP* mice were treated with vehicle, CL316,243 alone, the BA sequestrant Colesevelam alone to inhibit intestinal BA reabsorption, or the combination of both for a period of 4 or 12 weeks.

Material and methods

Additional detailed materials and methods are included in the **Supplemental methods**.

Animals and treatments

Hemizygous *APOE*3-Leiden* (*E3L*) mice were crossbred with homozygous human cholesteryl ester transfer protein (CETP) transgenic mice to generate heterozygous *E3L.CETP* mice [21]. At the age of 10-12 weeks, female mice were fed a Western-type diet (WTD; Altromin, Germany) containing 15% cacao butter, 1% corn oil and 0.15% (w/w) cholesterol.

In a first experiment [17], mice were randomized into 2 groups after a run-in period of 6 weeks on WTD. Mice were subsequently treated 5 days/week with the selective β3-AR agonist CL316,243 (symbol: β; Tocris Bioscience Bristol, United Kingdom; 20 $\mu g \cdot mouse^{-1}$) or vehicle (phosphate-buffered saline, symbol: -) by subcutaneous injections between 14:00 and 16:00 h for an additional 9 weeks.

In a second experiment, mice were randomized into 2 groups after a run-in period of 3 weeks on WTD and subsequently received WTD supplemented without or with 0.15% (w/w) Colesevelam (symbol: c; Genzyme Europe B.V., The Netherlands). After an additional run-in period of 3 weeks, mice in each treatment group were again randomized into 2 subgroups and additionally treated 5 days/week with vehicle or CL316,243 by subcutaneous injection for additional 4 weeks. This resulted in the following 4 treatment groups: 1) vehicle (-), 2) CL316, 243 (β), 3) Colesevelam (c), 4) Colesevelam + CL316, 243 (c+β).

In a third experiment, the set-up was similar to the second experiment, with the exception that mice were treated with CL316,243 or vehicle for 12 weeks.

Food intake and body weight were monitored weekly. Body composition (i.e. body fat and lean mass; EchoMRI-100; EchoMRI, Houston, TX, USA) was evaluated every two weeks. At the end of each experiment, mice were euthanized by CO_2 suffocation and unconscious mice were perfused with ice-cold saline via cardiac perfusion, and various organs were isolated for further analysis.

These animal experiments were approved by the Animal Ethical Committee of Leiden University Medical Center, Leiden, The Netherlands (DEC 12252-02). All animal procedures were performed conform to the guidelines from Directive 2010/63/EU of the European

Parliament on the protection of animals used for scientific purposes.

Fecal and plasma bile acid analysis

Feces were collected over a 24-hour period and dried at room temperature, weighed and homogenized. Bile acid (BA) composition was determined in an aliquot of feces by gas liquid chromatography (GC). Plasma BA profile was measured using liquid chromatography tandem MS (LC-MS/MS).

Biliary bile acid collection and composition analysis

Mice were anesthetized by intraperitoneal injection with Hypnorm (1 $mL \cdot kg^{-1}$; Janssen Pharmaceuticals) and Diazepam (10 $mg \cdot kg^{-1}$; Actavis). The bile duct was ligated and the gallbladder was cannulated to collect BAs. Hepatic bile was collected for 15 min and the average of bile flow per minute was calculated. BA compositions were determined in 5 **µL** bile by GC as described above. Biliary cholesterol levels were determined using an enzymatic kit from Roche Diagnostics (Mannheim, Germany).

Gene expression analysis

Gene expression analysis was performed as described in the Supplementary material. The primer sequences used are listed in Supplemental table 1.

Plasma lipid assays and lipoprotein profiles

Plasma was assayed for TG and total cholesterol (TC) using enzymatic kits from Roche Diagnostics (Mannheim, Germany) as described in the Supplementary material. The distribution of TG and cholesterol over lipoproteins was determined in pooled plasma by fast-performance liquid chromatography (FPLC) using a Superose 6 column (GE Healthcare, Piscataway, NJ).

Hepatic lipid content

Liver lipids were assayed as described in the Supplementary material.

***In vivo* plasma decay and hepatic uptake of TG-rich lipoprotein-like particles**

TG-rich lipoprotein (TRL)-like particles (80 nm), double-labeled with glycerol tri[^{3}H]oleate ([^{3}H]TO) and [^{14}C]cholesteryl oleate ([^{14}C]CO), were prepared as described previously [22]. Mice were fasted for 4 h and injected (t = 0) intravenously with 200 µL of TRL-like particles (1 mg TG per mouse). Blood samples were taken from the tail vein at 2, 5, 10 and 15 min after injection to determine the plasma decay of [^{3}H]TO and [^{14}C]CO. After 15 min, livers were isolated and weighted, and ^{3}H- and ^{14}C-activity were quantified.

Atherosclerosis quantification

Hearts were collected, fixed in phosphate-buffered 4% formaldehyde, and embedded in paraffin. Four sections of the aortic root area with 50 µm-intervals were used and stained with haematoxylin-phloxine-saffron for histological analysis. Lesions were categorized for lesion severity according to the guidelines of the American Heart Association adapted for mice [23] and classified as mild lesions (types 1 - 3) and severe lesions (types 4 - 5). Monoclonal mouse antibody M0851 against smooth muscle cell (SMC) actin was used to quantify the SMC area, Sirius Red staining was used to quantify the collagen area, and rat monoclonal antibody MAC3 was used to quantify macrophage area as described [17]. Lesion area was determined with Image J Software (version 1.50i).

Statistical analysis

Differences between two groups were determined using the unpaired two-tailed Student's t-test. Differences between four groups were determined using one-way ANOVA with the LSD posthoc test, which however increases the alpha risk as it does not correct for multiple comparisons. The square root of the lesion area was transformed to linearize the relationship with the plasma TC exposure. Univariate regression of analyses was performed to test for significant correlations between atherosclerotic lesion area and plasma TC exposure. Multiple regression analysis was performed to predict the contribution of plasma TC exposures to the atherosclerotic lesion area. Probability values less than 0.05 were considered statistically significant. All statistical analyses were performed with the GraphPad Prism 7 for Windows.

Results

Prolonged β3-AR agonism decreases fecal bile acid excretion and increases plasma bile acid levels

We previously fed female *E3L.CETP* mice a WTD and treated them with the β3-AR agonist CL316,243 (β) or vehicle (-) for 9 weeks, and observed that prolonged β3-AR agonism significantly increases liver TC levels [17]. Since bile acid (BA) synthesis is the major route of hepatic cholesterol catabolism, we now analyzed BAs level in feces and plasma of this 9 weeks treatment study [17]. Notably, prolonged β3-AR agonism reduced fecal total BA output into feces (-31%; **Figure 1A**), which equals hepatic BA synthesis rate under steady-state conditions. While fecal CA-derived BA secretion only tended to be reduced (-27%, *P*=0.07; **Figure 1B**), fecal CDCA-derived BA secretion was significantly reduced (-35%; **Figure 1C**). The fecal excretion of secondary BAs was unaffected (**Figure 1D**). In plasma, total BA levels were markedly increased (+258%; **Figure 1E**) and this was due to an increase in both CA-derived BAs (+295%; **Figure 1F**) and CDCA-derived BAs (+217%; **Figure 1G**). β3-AR agonism also increased plasma secondary BA levels (+33%, **Figure 1H**), and the proportion of conjugated BAs (+55%, **Supplemental figure 1A**). Collectively, these data suggest that prolonged β3-AR agonism decreases fecal BA output related to stimulation of BA reuptake.

Prolonged β3-AR agonism reduces the expression of genes involved in bile acid synthesis.

To further reveal how β3-AR agonism regulates BA metabolism, hepatic mRNA expression of genes involved in BA metabolism was investigated. While β3-AR agonism only tended to reduce *Cyp7a1,* it significantly reduced *Hsd3b7* (-57%) and *Cyp8b1* (-40%) (**Supplemental figure 1B**), all of which are involved in the classical BA synthesis pathway. In addition, β3-AR agonism reduced *Cyp27a1* (-53%) and *Cyp7b1* (-38%) (**Supplemental figure 1C**), which are involved in the alternative BA synthesis pathway. This data is consistent with the reduced fecal BA excretion, implying a reduced hepatic BA synthesis rate under steady-state conditions. β3-AR agonism also tended to reduce *Abcg5* (-31%, *P*=0.06) and *Bsep* expression (-27%, *P*=0.05) (**Supplemental figure 1D**), involved in excretion towards the bile of sterols and BAs, respectively. On the other hand, β3-AR agonism increased expression of *Ost-β* (+64%; **Supplemental figure 1E**), involved in the basolateral BA secretion from the liver towards the systemic circulation. β3-AR agonism tended to reduce *Oatp1a1* expression (-60%, *P*=0.06) and significantly reduced *Ntcp* expression (-37%) (**Supplemental figure 1F**), involved in the uptake of reabsorbed BAs by the liver.

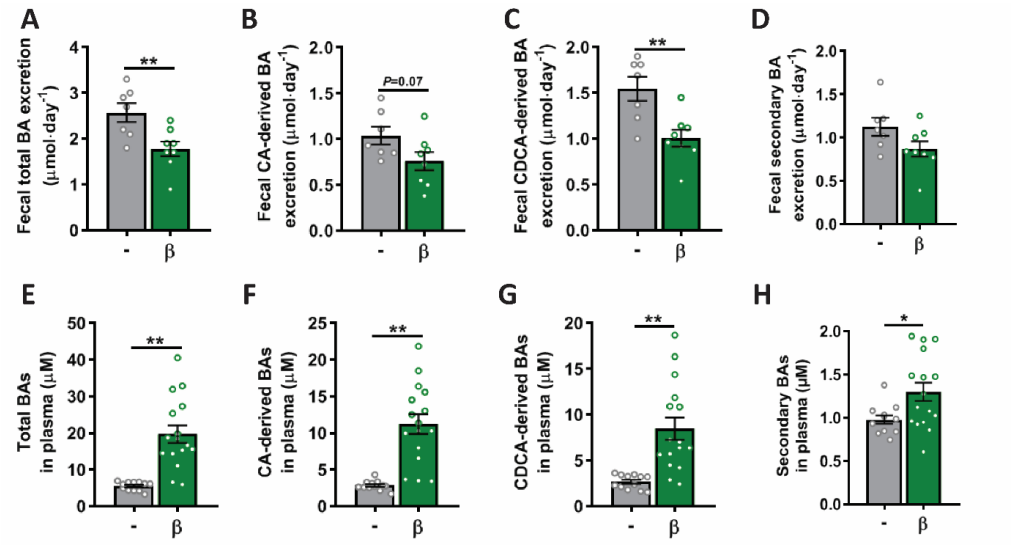

Figure 1. Prolonged β3-AR **agonism decreases fecal bile acid excretion and increases plasma bile acid levels.** *E3L.CETP* mice fed a WTD were treated with the β3-AR agonist CL316,243 (β) or vehicle (-) for 9 weeks. During the last week of treatment, feces were collected, and BA species were assayed. Fecal excretion of (**A**) total bile acid (BAs), (**B**) cholic acid (CA)-derived BAs, (**C**) chenodeoxycholic acid (CDCA)-derived BAs, and (**D**) secondary BAs were calculated; n= 7-8 mice/ group. Plasma was collected and (**E**) total BAs, (**F**) CA-derived BAs, (**G**) CDCA-derived BAs and (H) secondary BAs were determined; n= 14-16 mice/ group. Values are means ± SEM. Differences were determined using the unpaired two-tailed Student's t-test. **P*<0.05, ***P*<0.01, ****P*<0.001 vs vehicle (–).

Bile acid sequestration reverses β3-AR-mediated reduction of fecal bile acid output and normalizes elevated plasma bile acid levels

Because we observed that β3-AR agonism decreases fecal BA excretion and increases plasma BAs, we next assessed whether inhibition of intestinal BA reabsorption, by using the BA sequestrant Colesevelam, would stimulate fecal BA loss and prevent the increase in plasma BAs during prolonged β3-AR agonism. Mice were treated for 4 weeks with vehicle, the β3-AR agonist alone, a low dose of the BA sequestrant alone (Colesevelam 0.15% in the WTD, w/w), or the combination of β3-AR agonism and BA sequestration. β3-AR agonism, Colesevelam, or the combination did not influence food intake (**Supplemental figure 2A**), body weight (**Supplemental figure 2B**), or body lean mass (**Supplemental figure 2C**). As expected, β3-AR agonism tended to reduce body fat mass (*P*=0.09; **Supplemental figure 2D**) and significantly reduced gonadal white adipose tissue weight (gWAT; **Supplemental figure 2E**). The combination of β3-AR agonism and BA sequestration significantly reduced body fat mass (**Supplemental figure 2D**) and gWAT weight (**Supplemental figure 2E**) as compared to vehicle. Liver weight was not significantly influenced by β3-AR agonism alone or in combination with BA sequestration (**Supplemental figure 2F**).

Compared to vehicle, β3-AR agonism alone, BA sequestration alone, and the combination of β3-AR agonism and BA sequestration all increased bile flow (+43%, +33%, and +38% vs vehicle, respectively; **Figure 2A**). The biliary BA secretion rate was not influenced by the different treatments (**Figure 2B**). Additionally, biliary cholesterol excretion rate was increased

by β3-AR agonism (+75% vs vehicle), but not by BA sequestration or the combination of β3-AR agonism and BA sequestration (**Figure 2C**).

Furthermore, although 4-weeks β3-AR agonism did not significantly decrease fecal excretion of total BAs (**Figure 2D**) and CA-derived BAs (**Figure 2E**), excretion of CDCA-derived BAs was significantly decreased (-50% vs vehicle; **Figure 2F**). BA sequestration on top of β3-AR agonism strongly increased fecal excretion of total BAs (+91% vs vehicle; +234% vs β; +47% vs c; **Figure 2D**), CA-derived BAs (+201% vs vehicle; +357% vs β; **Figure 2E**) and CDCA-derived BAs (+109% vs β; **Figure 2F**). In addition, BA sequestration on top of β3-AR agonism markedly increased fecal secondary BA excretion (+122% vs vehicle; +274% vs β; +40% vs c; **Figure 2G**). Finally, although the β3-AR agonism-induced increase in plasma BA levels was not as pronounced as after 9 weeks of treatment, concomitant BA sequestration normalized these plasma BA levels (**Figure 2H-J**). β3-AR agonism clearly increased plasma secondary BA levels (+63% vs vehicle), which was completely reversed by BA sequestration (-118% vs c+ **β; Figure 2K**). Taken together, these data indicate that inhibition of BA reabsorption by BA sequestration reverses β3-AR agonism-induced reduction of fecal BA excretion, i.e., stimulates hepatic BA synthesis under these conditions, and normalizes β3-AR agonism-mediated increased plasma BA levels.

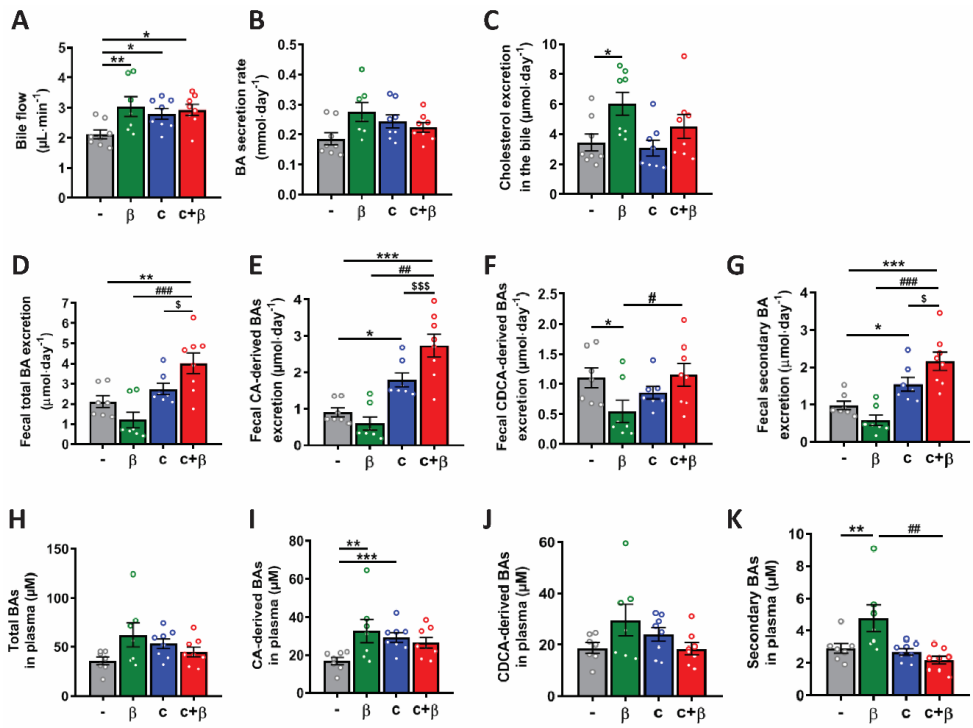

Figure 2. Bile acid sequestration reverses β3-AR induced reduction of fecal bile acid excretion and normalizes elevated plasma bile acid levels. *E3L.CETP* mice fed a WTD were treated with vehicle (-), the β3-AR agonist CL316,243 (β), the bile acid (BA) sequestrant Colesevelam (c), or their combination (c+β) for 4 weeks. Bile duct cannulation was performed to collect the bile and (**A**) bile flow (µL per minute) was determined. (**B**) BA secretion rate and (**C**) cholesterol excretion rate in the bile were determined. Feces were collected to determine fecal (**D**) total BAs, (**E**) cholic acid (CA)-derived BAs, (**F**) chenodeoxycholic acid (CDCA)-derived BAs, and (**G**) secondary BAs. In plasma, (**H**) total BAs, (**I**) CA-derived BAs, (**J**)

CDCA-derived BAs, and (**K**) secondary BAs were determined. N= 7-8 mice/ group. Values are means ± SEM. Differences between 4 groups were determined using one-way ANOVA with the LSD posthoc test. **P*<0.05, ***P*<0.01, ****P*<0.001 vs vehicle (-); $^{\#}$*P*<0.05, $^{\#\#}$*P*<0.01, $^{\#\#\#}$*P*<0.001 vs β3-AR agonist (β); $^{\$}$*P*<0.05, $^{\$\$\$}$*P*<0.001 vs Colesevelam (c).

Bile acid sequestration on top of β3-AR agonism reverses hepatic cholesterol accumulation and further improves plasma cholesterol levels

As the BA sequestrant Colesevelam on top of β3-AR agonism strongly increased fecal BA excretion and normalized plasma BA levels, we evaluated whether the addition of BA sequestration could also correct the β3-AR agonism-induced hepatic cholesterol accumulation as shown previously [17] and further lower plasma lipids. We confirmed that β3-AR agonism significantly increased hepatic TC levels (+26%). BA sequestration alone reduced hepatic TC levels as compared to vehicle (-41%) (**Figure 3A**). Importantly, BA sequestration on top of β3-AR agonism also largely reduced hepatic TC levels as compared to vehicle (-37%) and β3-AR agonism alone (-50%) (**Figure 3A**), and to similar levels as BA sequestration alone. Hepatic TG and PL contents were not influenced by any of the treatments (**Figure 3B and 3C**).

Next, we assessed the effect of BA sequestration on top of β3-AR agonism on plasma lipid levels. After 4 weeks of treatment, plasma TG levels were reduced by β3-AR agonism (-52%) and tended to be reduced by BA sequestration alone (-33%, *P*=0.07) as compared to vehicle. BA sequestration on top of β3-AR agonism reduced plasma TG levels as compared to vehicle (-74%) and also as compared to BA sequestration alone (-62%) (**Figure 3D**). In addition, BA sequestration alone reduced plasma TC levels as compared to vehicle (-47%). BA sequestration on top of β3-AR agonism also reduced plasma TC levels as compared to vehicle (-55%) and to β3-AR agonism alone (-49%; **Figure 3E**).

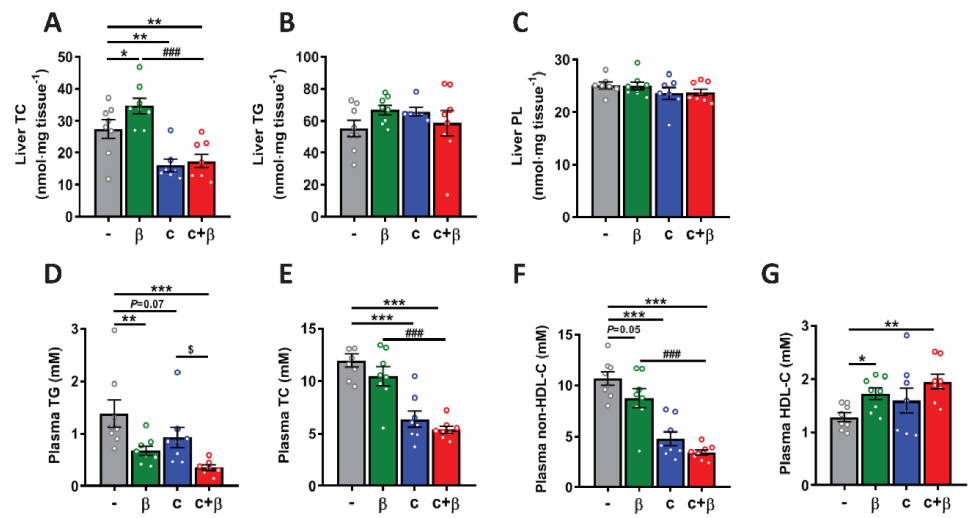

Figure 3. Bile acid sequestration on top of β3-AR agonism reverses hepatic cholesterol accumulation and further improves plasma cholesterol levels. *E3L.CETP* mice fed a WTD were treated with vehicle (-), β3-AR agonist CL316,243 (β), bile acid sequestrant Colesevelam (c), or their combination (c+β). After 4 weeks treatment, mice were killed and liver samples

were collected to evaluate hepatic (**A**) total cholesterol (TC), (**B**) triglyceride (TG), and (**C**) phospholipid (PL) levels. Blood samples were collected and plasma was assayed for (**D**) TG, (**E**) TC, and (**F**) non-HDL-cholesterol (non-HDL-C), and (**G**) HDL-cholesterol (HDL-C) levels. N= 7-8 mice/ group. Values are means ± SEM. Differences between 4 groups were determined using one-way ANOVA with the LSD posthoc test. **P*<0.05, ***P*<0.01, ****P*<0.001 vs vehicle (-); $^{\#\#\#}P$<0.001 vs β3-AR agonist (β); $^{\$}P$<0.05 vs Colesevelam (c).

Since cholesterol can be carried in plasma by either pro- or atherogenic lipoprotein classes, we also determined the distribution of cholesterol over plasma non-HDL and HDL. Plasma non-HDL-C levels tended to be reduced by β3-AR agonism alone (-27%, *P*=0.05), and were significantly reduced by BA sequestration alone (-55%) and BA sequestration on top of β3-AR agonism (-68%; **Figure 3F**) as compared to vehicle. Moreover, BA sequestration on top of β3-AR agonism further reduced non-HDL-C levels as compared to β3-AR agonism alone (-56%; **Figure 3F**). In addition, both β3-AR agonism alone (+34%), and in combination with BA sequestration (+52%; **Figure 3G**) increased anti-atherogenic HDL-C levels as compared to vehicle. Taken together, these findings indicate that BA sequestration on top of β3-AR agonism reverses the β3-AR agonism-induced hepatic cholesterol accumulation and further reduces plasma non-HDL-C levels.

Bile acid sequestration does not interfere with the β3-AR agonism-induced plasma clearance and hepatic uptake of cholesterol-enriched TRL remnants

As β3-AR agonism increases the formation and hepatic uptake of cholesterol-enriched TRL remnants [7, 17] and BA sequestration on top of β3-AR agonism further lowers plasma non-HDL-C levels, we next studied whether BA sequestration on top of β3-AR agonism influenced the hepatic uptake of cholesterol-enriched TRL remnants. Hereto, we treated mice with the BA sequestrant Colesevelam on top of the β3-AR agonist CL316,243 for 12 weeks. Similar as in the 4-weeks study, β3-AR agonism alone and in combination with BA sequestration, but not BA sequestration alone, reduced body fat mass (-37% and -38%, respectively; **Supplemental Figure 3A**) and gWAT weight (-55% and -61%, respectively; **Supplemental Figure 3B**) as compared to vehicle. In agreement with previous studies [7, 17], we also observed that β3-AR agonism induced substantial brown fat activation and browning of WAT as evidenced from decreased lipid contents in BAT (**Supplemental Figure 3C**) and subcutaneous WAT (scWAT, **Supplemental Figure 3D**), while BA sequestration on top of β3-AR agonism did not further add to these effects. The mRNA expression of genes related to intestinal BA reabsorption in the ileum is shown in **Supplemental Table 2**. β3-AR agonism significantly increased the mRNA expression of BA transporters *Asbt* and *Ost-β*. Furthermore, β3-AR agonism markedly increased *Shp* and *Fgf15* mRNA expression in the ileum, while the expression of these genes was reduced by BA sequestration, and normalized by the combination treatment.

In line with the 4-weeks intervention, 12 weeks of β3-AR agonism alone improved dyslipidemia by reducing plasma TG (-35%; **Figure 4A**), mainly via reducing (V)LDL-TG (**Figure 4B**), TC (-31%; **Figure 4C**) and non-HDL-C (-45%; **Figure 4D**) levels as compared to vehicle, while increasing HDL-C levels (+52%; **Figure 4E**). The decrease in (V)LDL-C and increase in HDL-C by β3-AR agonism alone and on top of BA sequestration was confirmed by FPLC (**Figure 4F**). As compared to β3-AR agonism alone, BA sequestration on top of β3-AR agonism did not influence plasma TG (**Figure 4A**), but further lowered plasma TC (-24%; **Figure 4C**) and tended to further reduce non-HDL-C levels (-32%, *P* = 0.06; **Figure 4D**). Next, the total plasma TC and non-HDL-C exposure during the treatment period were calculated. The combination treatment further reduced both the total plasma TC exposure

(-18%; **Figure 4G**) and non-HDL-C exposure (-20%; **Figure 4H**) as compared to β3-AR agonism alone.

After 12 weeks of treatment we evaluated the plasma clearance and hepatic uptake of intravenously injected glycerol tri[^{3}H]oleate (triolein, TO) and [^{14}C]cholesteryl oleate (CO) double-labeled VLDL-mimicking particles. In line with previous studies [7, 17], β3-AR agonism alone markedly accelerated the plasma clearance of [^{3}H]TO-derived activity (**Figure 4I**) and [^{14}C]CO (**Figure 4J**), and increased the hepatic uptake of the formed cholesterol-enriched TRL remnants (+25%, **Figure 4K**) as compared to vehicle. Additional BA sequestration did not further accelerate the plasma clearance of [^{3}H]TO-derived activity and [^{14}C]CO and also did not further increase the hepatic uptake of [^{14}C]CO (**Figure 4I-K**) as compared to β3-AR agonism alone.

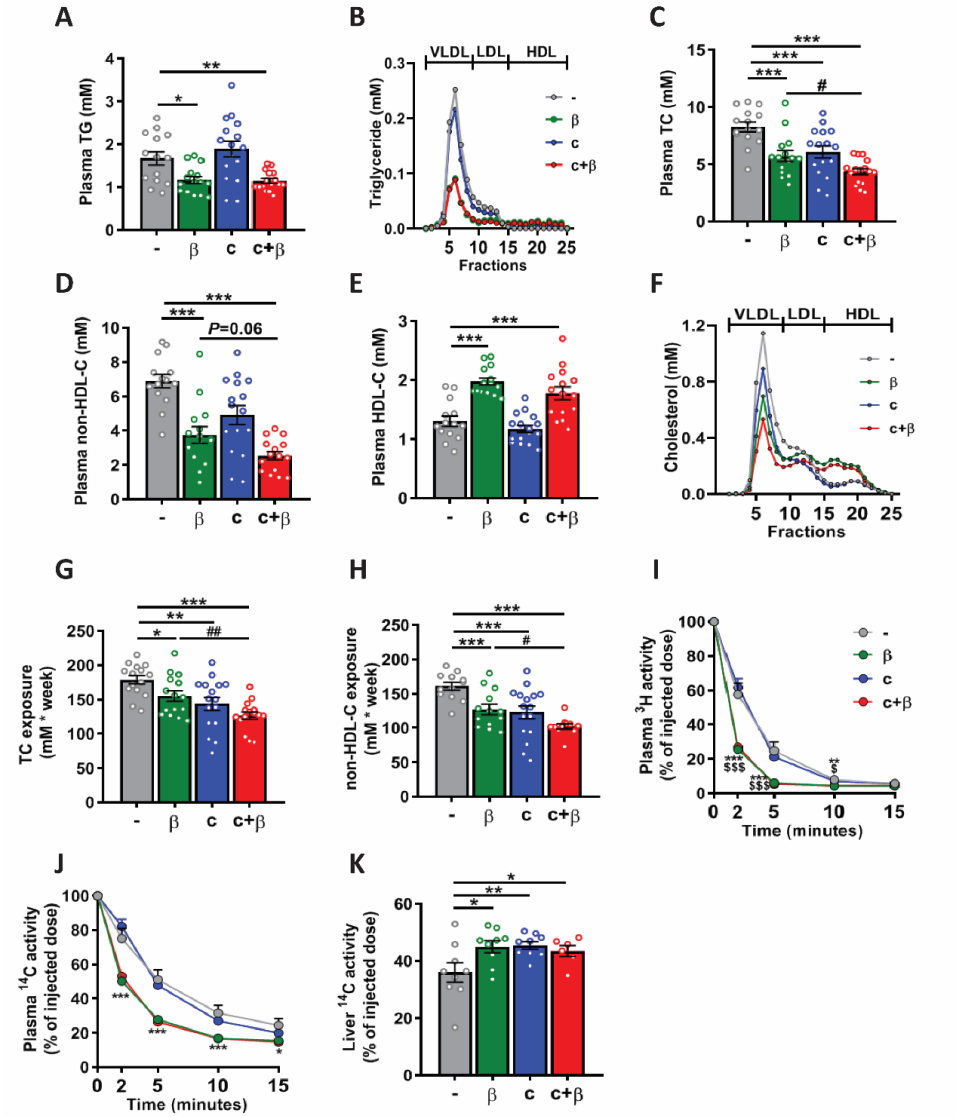

Figure 4. Bile acid sequestration does not interfere with the β3-AR agonism-induced plasma clearance and hepatic uptake of cholesterol-enriched TRL remnants. *E3L.*

CETP mice fed a WTD were treated with vehicle (-), the β3-AR agonist CL316,243 (β), the bile acid sequestrant Colesevelam (c), or their combination (c+β). After 12 weeks treatment, blood was collected to determine plasma (**A**) triglycerides (TG), (**B**) distribution of TG over lipoproteins, (**C**) total cholesterol (TC), (**D**) non-HDL-cholesterol (non-HDL-C), (**E**) HDL-cholesterol (HDL-C) and (**F**) distribution of TC over lipoproteins. (**G**) TC and (**H**) non-HDL-C exposure were calculated; n= 13-16 mice/ group. Mice were injected intravenously with glycerol tri[^{3}H]oleate and [^{14}C]cholesteryl oleate-labeled lipoprotein-like particles. Plasma clearance of (**I**) ^{3}H-activity and (**J**) ^{14}C-activity, and (**K**) hepatic uptake of ^{14}C-activity after 15 min were measured; n= 6-9 mice/ group. Values are means ± SEM. Differences between 4 groups were determined using one-way ANOVA with the LSD posthoc test. **P*<0.05, ***P*<0.01, ****P*<0.001 vs vehicle (-); $^{\#\#}$*P*<0.01 vs β3-AR agonist (β); $^{\$}$*P*<0.05, $^{\$\$\$}$*P*<0.001 vs Colesevelam (c).

Bile acid sequestration on top of β3-AR agonism tends to further **attenuate atherosclerosis development**

To investigate if the beneficial effects of BA sequestration on top of β3-AR agonism on BA and cholesterol metabolism would translate in a further protection against atherosclerosis development, we evaluated the atherosclerotic lesion area in the root of the aortic arch after 12 weeks of treatment. As expected, β3-AR agonism alone decreased atherosclerotic lesion area throughout the aortic root (**Figure 5A and 5B**), resulting in lower mean atherosclerotic lesion area as compared to vehicle (-56%; **Figure 5C**). BA sequestration on top of β3-AR agonism strongly attenuated atherosclerotic lesion area by -79% as compared to vehicle; and as compared to β3-AR agonism alone tended to further reduce the atherosclerotic lesion area (-54%; *P*=0.16) (**Figure 5C**). The total plasma TC exposure during the study strongly correlated with the square root (SQRT)-transformed lesion area (β=2.14, R^2=0.40; p<0.001; **Figure 5D**). Moreover, although atherosclerotic lesion severity was not significantly mitigated by any treatment (**Supplemental figure 4A**), β3-AR agonism increased the proportion of lesion-free valves as compared to vehicle (+122%), which was further increased by additional BA sequestration (+199% vs vehicle; +34% vs β; **Figure 5E**). Proportions of smooth muscle cell area and collagen area were not affected by any of the treatments (**Figure 5F, 5G and Supplemental figure 4B**), while BA sequestration on top of β3-AR agonism further decreased the percentage of macrophage area within the lesion (-34% vs vehicle; -26% vs β; **Figure 5H and Supplemental figure 4B**) and increased the stability index defined by the ratio of stable markers (i.e. smooth muscle cell area and collagen area) versus the unstable marker (i.e. macrophage area) (+70% vs vehicle; +44% vs β; **Figure 5I**).

Taken together, BA sequestration in addition to β3-AR agonism tends to further reduce atherosclerosis development, an effect that is strongly related to its plasma cholesterol-lowering effect.

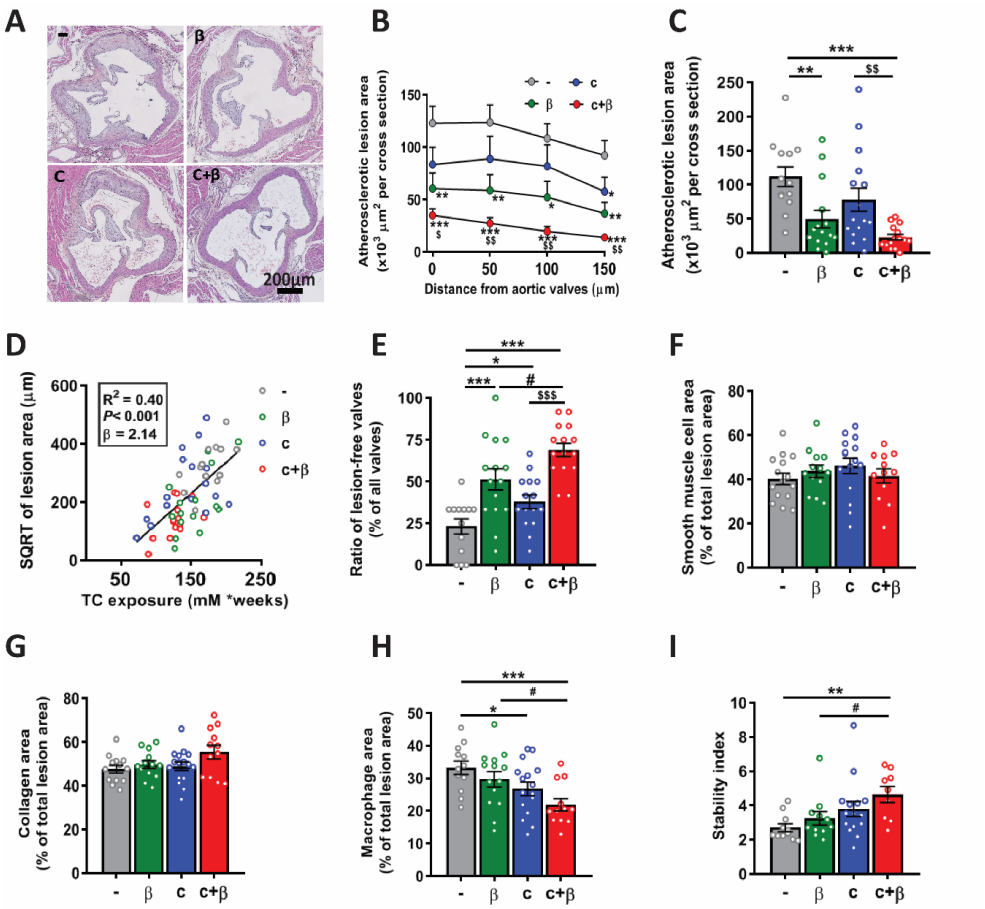

Figure 5. Bile acid sequestration on top of β3-AR agonism tends to further attenuate atherosclerosis development. *E3L.CETP* mice fed a WTD were treated with vehicle (-), the β3-AR agonist CL316,243 (β), the bile acid sequestrant Colesevelam (c), or their combination (c+β) for 12 weeks. (**A**) Representative pictures of atherosclerotic lesions in aortic root area of each group are shown. (**B**) Plaque lesion area as a function of distance from the appearance of open valves and (**C**) mean atherosclerotic lesion area were calculated. (**D**) The square root (SQRT) of the mean atherosclerotic lesion area is plotted against the plasma total cholesterol (TC) exposure during the whole treatment period. (**E**) Ratio of the number of valves without any lesions divided by the total number of valves is shown. Relative areas of (**F**) smooth muscle cells, (**G**) collagen, and (**H**) macrophages within the lesion were determined. (**I**) The stability index was calculated as the ratio of stable markers (i.e. smooth muscle cell area and collagen area) per unstable marker (i.e. macrophage area). N= 13-16 mice/ group. Values are means ± SEM. Differences between 4 groups were determined using one-way ANOVA with the LSD posthoc test. **P*<0.05, ***P*<0.01, ****P*<0.001 vs vehicle (-); $^{\#}$*P*<0.05 vs β3-AR agonist (β); $^{\$}$*P*<0.05, $^{\$\$}$*P*<0.01, $^{\$\$\$}$*P*<0.001 vs Colesevelam (c).

Discussion

Activating brown fat is a promising strategy to combat hypercholesterolemia by increasing the flux of lipoprotein-associated cholesterol towards the liver, thereby exerting atheroprotective effects [7, 9]. The aim of this study was first to evaluate the effects of prolonged brown fat activation, via β3-AR agonism, on hepatic cholesterol turnover. Secondly we aimed to assess the effects of BA sequestration on top of brown fat activation on hepatic cholesterol and BA metabolism as well as atherosclerosis development. We uncovered that the increased hepatic cholesterol content by prolonged β3-AR agonism as shown previously [17], was accompanied by increased plasma BA levels and decreased fecal BA excretion. It is likely that more efficient BA reabsorption from the gut is mostly responsible for these effects, since biliary BA (representing both newly synthesized BAs and cycled BAs within the enterohepatic circulation) output was actually increased under these conditions. Indeed, concomitant BA sequestration by Colesevelam markedly increased fecal BA excretion and lowered the hepatic cholesterol content. As a result, combining BA sequestration with β3-AR agonism further reduced plasma cholesterol levels and tended to further reduce atherosclerosis development and also increase plaque stability as compared to β3-AR agonism alone.

Previously, we observed that prolonged β3-AR agonism in mice increases the delivery of cholesterol to the liver via the uptake of cholesterol-enriched TRL remnants [7] and HDL-C [9] and this increased flux of cholesterol towards the liver results in a moderate hepatic cholesterol accumulation [17]. In fact, 4 weeks of β3-AR agonism already clearly increased the hepatic cholesterol level. In the current study, we further show that prolonged β3-AR agonism decreased fecal BA excretion and increased plasma BA levels. Since there is negligible excretion of BAs via the urine and skin, hepatic BA synthesis from cholesterol equals fecal BA excretion under steady-state conditions to maintain BA pool size [24]. Our data therefore demonstrate that prolonged β3-AR agonism decreases hepatic BA synthesis in mice. This is supported by the reduced expression of genes involved in the classical and alternative BA synthesis pathways. The observation that the biliary BA secretion rate was not decreased after prolonged β3-AR agonism, but rather tended to be increased, can be explained by the fact that the biliary BAs represent both newly synthesized BAs as well as BAs that are recycled within the enterohepatic circulation. β3-AR agonism increases BA reabsorption from the gut (i.e. increasing cycled BAs within the enterohepatic circulation), which is responsible for the overall increased biliary BA output. In line with our study, Baskin *et al.* recently showed that the β3-AR agonist mirabegron increased gallbladder size in humans [25], which could be caused by an increased BA-induced bile flow upon brown fat activation.

The current study shows that the effects of prolonged brown fat activation on BA metabolism partly differ from the effects of short-term brown fat activation. Previous observations by us and others with short-term brown fat activation by means of β3-AR agonism and cold exposure (*i.e.* 1 week) showed increased expression of genes related to BA synthesis [18] and increased fecal BA excretion [9, 18]. This difference observed with treatment duration is likely explained by an initial transient induction of BA synthesis upon brown fat activation, that is driven by the increased hepatic influx of cholesterol, the main substrate for BA synthesis [26], and dependent on hepatic induction of Cyp7b1[18]. After prolonged brown fat activation, the higher concentration of BAs in the gut likely stimulates BA reabsorption from the gut to prevent BA loss from the body. Subsequently, both BAs in the gut, via induction of FGF15 production, and circulating BAs target the hepatic FXR pathway and inhibit BA synthesis via a well-established feed-back mechanism [15]. Based on our findings, 4-weeks of β3-AR agonism is sufficient to induce such an inhibitory feedback on BA synthesis. Collectively, available data indicate that brown fat activation initially increases BA synthesis and thereby

fecal BA excretion, while prolonged brown fat activation, decreases hepatic BA synthesis and thereby induces hepatic cholesterol accumulation. It appears that under these conditions reabsorption of BAs from the gut becomes more efficient, which, possibly in combination with suppressed expression of hepatic BA uptake transporters, leads to elevated plasma levels of BAs. High hepatic cholesterol and BA levels may affect liver function by inducing liver inflammation [27, 28].

Since prolonged β3-AR agonism increased plasma levels of BAs, including secondary BAs, and decreased fecal BA excretion, we reasoned that prolonged β3-AR agonism induces reabsorption of BAs from the gut. In fact, β3-AR agonism clearly increased the expression of Asbt, the predominant transporter for the uptake of the luminal Bas [29], and Ost-β, a basolateral BA transporter which plays a key role in BA efflux in the ileum[30, 31]. In addition to increasing the expression of BA transporters, β3-AR agonism increased plasma secondary BA levels. Intestinal anaerobic bacteria, *i.e.* Eubacterium and Clostridium [32] are capable to deconjugate the liver-derived BAs and convert primary BAs into secondary BAs, such as LCA (omega-MCA in mice) and DCA, which has a high affinity to ASBT in the ileum[33]. The activity of those obligatory anaerobic bacteria would be largely impaired when feces were collected and placed in the presence of oxygen. Thus, the effect of β3-AR agonism on increasing intestinal BA reabsorption may be attributed to upregulation of Asbt and Ost-β expression in the ileum as well as increased conversion of primary BAs into secondary BAs in the gut.

Colesevelam is a BA sequestrant that reduces the reabsorption of BAs from the gut, with a preference for relatively hydrophobic species like deoxycholic acid (DCA; *i.e.* the main secondary BA derived from CA) [26]. Likely via this mechanism, Colesevelam particularly increased fecal secondary BA excretion. Interruption of the enterohepatic circulation by a very low dosage of Colesevelam is not complete and increased hepatic synthesis and sufficient BAs within the circulation resulted in a similar biliary BA secretion rate and actually a slightly increased bile flow as compared to vehicle, which corroborates previous studies [34, 35]. Most importantly and fully in line with our expectations, Colesevelam strongly decreased levels of both hepatic and plasma cholesterol, explained by the fact that BA elimination is by far the most important contributor to cholesterol turnover [26]. The β3-AR agonism-induced BA reabsorption is likely effectively inhibited by BA sequestration, as Colesevelam on top of β3-AR agonism markedly increased fecal excretion of total BAs and secondary BAs. As a consequence of prevention of reabsorption, plasma BA levels, in particular secondary BAs were normalized upon BA sequestration on top of β3-AR agonism. The fact that BA sequestration on top of β3-AR agonism still lowered hepatic cholesterol to similar levels as reached by BA sequestration alone indicates that the effects of BA sequestration on hepatic cholesterol levels and BA synthesis is stronger than the effects of β3-AR agonism.

Preclinical studies showed that both β3-AR agonism alone [7, 17] and the BA sequestrant Colesevelam alone [35] not only reduce plasma cholesterol levels but also atherosclerosis development. Importantly, we now show that BA sequestration on top of β3-AR agonism further reduces plasma non-HDL-C levels, tended to further reduce atherosclerosis development and further increased plaque stability as evidenced by reduced macrophage area *versus* smooth muscle cell and collagen area within the lesion. This finding is highly relevant from a clinical perspective. In humans the β3-AR agonist Mirabegron increases brown fat activity and resting energy expenditure [36] and high brown fat activity is associated with a reduced risk of cardiovascular disease events [37]. In addition, BA sequestrants attenuate coronary heart disease and coronary artery lesions in humans [38]. Based on our findings, we speculate that combining conventional lipid-lowering by BA sequestration with brown fat

activation may further improve dyslipidemia and reduce atherosclerosis development in clinic.

In conclusion, prolonged β3-AR agonism promotes BA reabsorption from the gut, resulting in elevated plasma BA levels, suppressed hepatic BA synthesis and elevated hepatic cholesterol content. Concomitant BA sequestration on top of β3-AR agonism increases fecal BA excretion, normalizes plasma BA levels, reverses the β3-AR agonism-induced hepatic cholesterol accumulation, further lowers plasma non-HDL-C levels and tends to further lower atherosclerosis development. These data suggest that combining conventional BA sequestration with brown fat activation via β3-AR agonism could be a new therapeutic strategy to further reduce dyslipidemia and attenuate atherosclerosis development.

Acknowledgements

This work was supported by the Netherlands Organisation for Scientific Research-NWO (VENI grant 91617027 to Y.W.); the Netherlands Organisation for Health Research and Development-ZonMW (Early Career Scientist Hotel grant 435004007 to Y.W.); EU research funding (FP7-HEALTH-305707 to A.K.G.); the Netherlands Cardiovascular Research Initiative: an initiative with support of the Dutch Heart Foundation (CVON-GENIUS-2); and the Netherlands Heart Foundation (grant 2009T038 to P.C.N.R). E.Z. is supported by the China Scholarship Council (CSC, grant 201606010321).

The authors thank Elsbeth J. Pieterman (TNO-Metabolic Health Research, Gaubius Laboratory, Leiden, The Netherlands) for technical assistance on the fast-performance liquid chromatography.

Author contributions

E.Z., G.H.: study concept and design; acquisition of data; analysis and interpretation of data; drafting of the manuscript; edited and revised manuscript; Z.L., A.C.E., A.W.S., R.H.H., M.K., R.B., F.K.: acquisition of data, edited and revised manuscript; T.C., M.R.B, J.F.P.B.: study concept and design, edited and revised manuscript; A.K.G., P.C.N.R.: study concept and design, obtained funding, study supervision, edited and revised manuscript; Y.W.: study concept and design; analysis and interpretation of data; drafting of the manuscript; edited and revised manuscript; obtained funding.

Conflict of interest

The authors report no declarations of interest.

References

1. Jukema, J.W., et al., *The controversies of statin therapy: weighing the evidence.* J Am Coll Cardiol, 2012. **60**(10): p. 875-81.
2. Ouellet, V., et al., *Brown adipose tissue oxidative metabolism contributes to energy expenditure during acute cold exposure in humans.* J Clin Invest, 2012. **122**(2): p. 545-52.
3. Labbe, S.M., et al., *In vivo measurement of energy substrate contribution to cold-induced brown adipose tissue thermogenesis.* FASEB J, 2015. **29**(5): p. 2046-58.
4. Oikonomou, E.K. and C. Antoniades, *The role of adipose tissue in cardiovascular health and disease.* Nat Rev Cardiol, 2019. **16**(2): p. 83-99.
5. Hoeke, G., et al., *Role of Brown Fat in Lipoprotein Metabolism and Atherosclerosis.* Circ Res, 2016. **118**(1): p. 173-82.
6. Cannon, B. and J. Nedergaard, *Brown adipose tissue: Function and physiological significance.* Physiological Reviews, 2004. **84**(1): p. 277-359.
7. Berbee, J.F., et al., *Brown fat activation reduces hypercholesterolaemia and protects from atherosclerosis development.* Nat Commun, 2015. **6**: p. 6356.
8. Khedoe, P.P., et al., *Brown adipose tissue takes up plasma triglycerides mostly after lipolysis.* J Lipid Res, 2015. **56**(1): p. 51-9.
9. Bartelt, A., et al., *Thermogenic adipocytes promote HDL turnover and reverse cholesterol transport.* Nat Commun, 2017. **8**: p. 15010.
10. Chiang, J.Y., *Regulation of bile acid synthesis: pathways, nuclear receptors, and mechanisms.* J Hepatol, 2004. **40**(3): p. 539-51.
11. Bjorkhem, I., et al., *Differences in the regulation of the classical and the alternative pathway for bile acid synthesis in human liver. No coordinate regulation of CYP7A1 and CYP27A1.* J Biol Chem, 2002. **277**(30): p. 26804-7.
12. de Boer, J.F., et al., *New insights in the multiple roles of bile acids and their signaling pathways in metabolic control.* Curr Opin Lipidol, 2018. **29**(3): p. 194-202.
13. Houten, S.M., *Homing in on bile acid physiology.* Cell Metab, 2006. **4**(6): p. 423-4.
14. Li, T. and J.Y. Chiang, *Bile acid signaling in metabolic disease and drug therapy.* Pharmacol Rev, 2014. **66**(4): p. 948-83.
15. Chiang, J.Y., *Bile acids: regulation of synthesis.* J Lipid Res, 2009. **50**(10): p. 1955-66.
16. *The Lipid Research Clinics Coronary Primary Prevention Trial results. I. Reduction in incidence of coronary heart disease.* JAMA, 1984. **251**(3): p. 351-64.
17. Hoeke, G., et al., *Atorvastatin accelerates clearance of lipoprotein remnants generated by activated brown fat to further reduce hypercholesterolemia and atherosclerosis.* Atherosclerosis, 2017. **267**: p. 116-126.
18. Worthmann, A., et al., *Cold-induced conversion of cholesterol to bile acids in mice shapes the gut microbiome and promotes adaptive thermogenesis.* Nat Med, 2017. **23**(7): p. 839-849.
19. van Vlijmen, B.J., et al., *Diet-induced hyperlipoproteinemia and atherosclerosis in apolipoprotein E3-Leiden transgenic mice.* J Clin Invest, 1994. **93**(4): p. 1403-10.
20. de Haan, W., et al., *Torcetrapib does not reduce atherosclerosis beyond atorvastatin and induces more proinflammatory lesions than atorvastatin.* Circulation, 2008. **117**(19): p. 2515-22.
21. Westerterp, M., et al., *Cholesteryl ester transfer protein decreases high-density lipoprotein and severely aggravates atherosclerosis in APOE*3-Leiden mice.* Arterioscler Thromb Vasc Biol, 2006. **26**(11): p. 2552-9.
22. Rensen, P.C., et al., *Selective liver targeting of antivirals by recombinant*

chylomicrons--a new therapeutic approach to hepatitis B. Nat Med, 1995. **1**(3): p. 221-5.
23. Wong, M.C., et al., *Hepatocyte-specific IKKbeta expression aggravates atherosclerosis development in APOE*3-Leiden mice.* Atherosclerosis, 2012. **220**(2): p. 362-8.
24. Hofmann, A.F. and L.R. Hagey, *Key discoveries in bile acid chemistry and biology and their clinical applications: history of the last eight decades.* J Lipid Res, 2014. **55**(8): p. 1553-95.
25. Baskin, A.S., et al., *Regulation of Human Adipose Tissue Activation, Gallbladder Size, and Bile Acid Metabolism by a beta3-Adrenergic Receptor Agonist.* Diabetes, 2018.
26. Kuipers, F., V.W. Bloks, and A.K. Groen, *Beyond intestinal soap--bile acids in metabolic control.* Nat Rev Endocrinol, 2014. **10**(8): p. 488-98.
27. Allen, K., H. Jaeschke, and B.L. Copple, *Bile acids induce inflammatory genes in hepatocytes: a novel mechanism of inflammation during obstructive cholestasis.* Am J Pathol, 2011. **178**(1): p. 175-86.
28. Tall, A.R. and L. Yvan-Charvet, *Cholesterol, inflammation and innate immunity.* Nat Rev Immunol, 2015. **15**(2): p. 104-16.
29. Kullak-Ublick, G.A., B. Stieger, and P.J. Meier, *Enterohepatic bile salt transporters in normal physiology and liver disease.* Gastroenterology, 2004. **126**(1): p. 322-42.
30. Dawson, P.A., et al., *The heteromeric organic solute transporter alpha-beta, Ostalpha-Ostbeta, is an ileal basolateral bile acid transporter.* J Biol Chem, 2005. **280**(8): p. 6960-8.
31. Rao, A., et al., *The organic solute transporter alpha-beta, Ostalpha-Ostbeta, is essential for intestinal bile acid transport and homeostasis.* Proc Natl Acad Sci U S A, 2008. **105**(10): p. 3891-6.
32. Wahlstrom, A., et al., *Intestinal Crosstalk between Bile Acids and Microbiota and Its Impact on Host Metabolism.* Cell Metab, 2016. **24**(1): p. 41-50.
33. Craddock, A.L., et al., *Expression and transport properties of the human ileal and renal sodium-dependent bile acid transporter.* Am J Physiol, 1998. **274**(1): p. G157-69.
34. Herrema, H., et al., *Bile salt sequestration induces hepatic de novo lipogenesis through farnesoid X receptor- and liver X receptor alpha-controlled metabolic pathways in mice.* Hepatology, 2010. **51**(3): p. 806-16.
35. Meissner, M., et al., *Bile acid sequestration normalizes plasma cholesterol and reduces atherosclerosis in hypercholesterolemic mice. No additional effect of physical activity.* Atherosclerosis, 2013. **228**(1): p. 117-23.
36. Cypess, A.M., et al., *Activation of human brown adipose tissue by a beta3-adrenergic receptor agonist.* Cell Metab, 2015. **21**(1): p. 33-8.
37. Takx, R.A., et al., *Supraclavicular Brown Adipose Tissue 18F-FDG Uptake and Cardiovascular Disease.* J Nucl Med, 2016. **57**(8): p. 1221-5.
38. Brensike, J.F., et al., *Effects of therapy with cholestyramine on progression of coronary arteriosclerosis: results of the NHLBI Type II Coronary Intervention Study.* Circulation, 1984. **69**(2): p. 313-24.

Supplemental appendix

Supplemental materials and methods

Animals and treatments

Hemizygous *APOE*3-Leiden* (*E3L*) mice were crossbred with homozygous human cholesteryl ester transfer protein (CETP) transgenic mice to generate heterozygous *E3L.CETP* mice [1]. Mice were housed under standard conditions with a 12-hours light/dark cycle, at room temperature (22°C) and with *ad libitum* access to food and water, unless indicated otherwise. At the age of 10-12 weeks, female mice were fed a Western-type diet (WTD; Altromin, Germany) containing 15% cacao butter, 1% corn oil and 0.15% (w/w) cholesterol.

In a first experiment [2], mice were randomized into 2 groups (based on plasma lipid levels, fat mass and age) after a run-in period of 6 weeks on WTD. Mice were subsequently treated 5 days/week with the selective β3-AR agonist CL316,243 (symbol: β; Tocris Bioscience Bristol, United Kingdom; 20 μg·mouse^{-1}) or vehicle (Phosphate-buffered saline, PBS, symbol -) by subcutaneous injections between 14:00 and 16:00 h for an additional 9 weeks.

In a second experiment, mice were randomized into 2 groups (based on plasma lipid levels, fat mass and age) after a run-in period of 3 weeks on WTD and subsequently received WTD supplemented without or with 0.15% (w/w) Colesevelam (symbol: c; Genzyme Europe B.V., The Netherlands). After an additional run-in period of 3 weeks, mice in each treatment group were again randomized into 2 subgroups (based on plasma lipid levels, fat mass and age) and additionally treated 5 days/week with vehicle (PBS, symbol -) or CL316,243 (symbol: β; 20 **μg**/mouse) by subcutaneous injection between 14:00 and 16:00 h for additional 4 weeks. This resulted in the following 4 treatment groups: 1) vehicle (-), 2) CL316, 243 (β), 3) Colesevelam (c), 4) Colesevelam + CL316, 243 (c+β).

In a third experiment, the set-up was similar to the second experiment, with the exception that mice were treated with vehicle or CL316,243 for 12 weeks.

Food intake and body weight were monitored weekly. Body composition (i.e. body fat and lean mass; EchoMRI-100; EchoMRI, Houston, TX, USA) was evaluated every two weeks. At the end of each experiment, mice were euthanized by CO_2 suffocation and unconscious mice were perfused with ice-cold saline via the cardiac perfusion, and various organs were isolated for further analysis.

These animal experiments (approval reference number DEC 12252-02) were approved by the Animal Ethical Committee of Leiden University Medical Center, Leiden, The Netherlands. All animal procedures performed conform to the guidelines from Directive 2010/63/EU of the European Parliament on the protection of animals used for scientific purposes.

Fecal and plasma bile acid analysis

In the last week of vehicle or CL316,243 treatment (first experiment: week 9; second experiment: week 4), feces were collected over a 24-hour period and dried at room temperature, weighed and homogenized. Bile acid (BA) composition was determined in an aliquot of feces by gas liquid chromatography (GC) as described previously [3-5] and modified as follows. Fecal BAs were solubilized from 50 mg feces in methanol/0.1 M sodium hydroxide (3:1) at 80°C for 2 h. As an internal standard 15 nmol of 5β-cholanic acid 7α,12α diol was added. Next, BAs were extracted using C-18 columns and eluted with 75% methanol followed evaporation at 65°C under a stream of nitrogen. Subsequently, BAs were deconjugated enzymatically by adding choloyl glycine hydrolase at 37°C for 15 h in sodium

acetate buffer pH 5.6. Next, BAs were extracted again using C-18 columns as described above. After drying the samples under nitrogen, the BAs were methylated using acetylchloride/ methanol at 55°C. Subsequently, a trimethylsilyl-derivative was made with N2O-bis/ trimethylsilyltrifluoroacetuylamide, pyridine and trimethylsilane. BAs were diluted in hexane and analyzed by GC (Agilent 6890, Amstelveen, The Netherlands) using a CPSil 19 capilliary column (25 m x 0.25 mm x 0.2 μm) (Chrompack, Middelburg, The Netherlands). Fecal BA and neutral sterol excretion were calculated accordingly.

After 9 weeks (the first experiment) or 4 weeks (the second experiment) CL316,243 or vehicle treatment, blood samples were collected from the tail vein to determine BA levels in plasma. An internal standard containing D4-cholate, D4-chenodeoxycholate, D4-glycocholate, D4-taurocholate, D4-glycochenodeoxycholate, D4-taurochenodeoxycholate, D4-tauroursodeoxycholate, D6-taurodeoxycholate and D4-tauro-beta-muricholate was added. Subsequently, samples were mixed and centrifuged at 15,900 g. The supernatant was removed, evaporated under vacuum at 40°C and reconstituted in 200 **μL** of 50% methanol. BA profile was measured using liquid chromatography tandem MS (LC-MS/MS) as described previously [6]. Cholic acid (CA)-derived BAs were calculated as the sum of CA, Taurocholic acid (TCA), Deoxycholic acid (DCA), Taurine (T) conjugated DCA (TDCA); chenodeoxycholic acid (CDCA)-derived BAs were calculated as the sum of CDCA, α-Muricholic acid (MCA), β-MCA, TCDCA, T-α-MCA, T-β-MCA, ω-MCA, T-ω-MCA, Ursodeoxycholic acid (UDCA), Hyodeoxycholic acid (HDCA), T-HDCA; secondary BAs were calculated as the sum of DCA, TDCA, UDCA, ω-MCA, T-ω-MCA, HDCA, THDCA.

Biliary bile acid collection and composition analysis

In the second experiment, after 4-weeks CL316,243 or vehicle treatment, mice were anesthetized by intraperitoneal injection with Hypnorm (1 $mL \cdot kg^{-1}$; Janssen Pharmaceuticals) and Diazepam (10 $mg \cdot kg^{-1}$; Actavis). The adequacy of anesthesia was confirmed by the lack of a toe-pinch withdrawal response during the surgical procedure. The bile duct was ligated and the gallbladder was cannulated to collect bile acids. During the collection period, body temperature was maintained with a heated mattress. Hepatic bile was collected for 15 min and the average of bile flow per minute was calculated. Bile acid compositions were determined in 5 **μL** bile by gas liquid chromatography (GC) as described previously [3-5] and modified as described above for plasma bile acid analysis. Biliary cholesterol levels were determined using an enzymatic kit from Roche Diagnostics (Mannheim, Germany).

Hepatic lipid content

After 4 weeks (the second experiment) of vehicle or CL316,243 treatment, mice were killed and pieces of liver were collected to extract liver lipids as previously described [7]. In brief, small liver pieces (approx. 50 mg) were homogenized in ice-cold methanol. 1,800 μL CH_3OH : $CHCl_3$ (1:3, v/v) was added to 45 μL homogenate. After vigorous vortexing and phase separation by centrifugation (18,800 g; 15 min at room temperature), the organic phase was dried and dissolved in 2% Triton X-100. TG, TC (both Roche Diagnostics, Mannheim, Germany) and phospholipid (Instruchemie, Delfzijl, The Netherlands) concentrations were measured using commercial kits. Liver lipids were expressed as $nmol \cdot mg^{-1}$ tissue.

Gene expression analysis

In the first experiment, after 9-weeks of vehicle or CL316,243 treatment, RNA was extracted from snap-frozen liver using Tripure RNA Isolation reagent (Roche Diagnostics) according to the manufacturer's protocol. Total RNA (1 μg) was reverse transcribed using Moloney Murine Leukemia Virus (M-MLV) Reverse Transcriptase (Promega) for RT-qPCR according

to the manufacturer's instructions to produce cDNA. mRNA expression was normalized to β2-microglobulin and *36b4* mRNA expression and expressed as fold change compared to vehicle-treated mice using the ΔΔCT method. The primer sequences used are listed in Supplemental table 1.

Plasma lipid assays and lipoprotein profiles

In all experiments blood was collected from the tail vein of 4 h-fasted mice into capillaries that were subsequently placed on ice and centrifuged. Plasma was assayed for TG and TC using enzymatic kits from Roche Diagnostics (Mannheim, Germany). To measure HDL-cholesterol (HDL-C) levels, apoB-containing lipoproteins were precipitated from plasma with 20% polyethylene glycol 6,000 in 200 mM glycine buffer (pH 10), and cholesterol was measured in the supernatant as described for TC. Plasma non-HDL-cholesterol (non-HDL-C) levels were calculated by subtraction of HDL-C from TC levels. Total TC and TG exposure was calculated as the area under the curve of plasma TC and TG over the complete treatment period. The distribution of TG and cholesterol over lipoproteins was determined in pooled plasma by fast-performance liquid chromatography (FPLC) using a Superose 6 column (GE Healthcare, Piscataway, NJ).

***In vivo* plasma decay and hepatic uptake of TG-rich lipoprotein-like particles**

At the end of the third experiment, after 12 weeks of treatment, TG-rich lipoprotein (TRL)-like particles (80 nm), double-labeled with glycerol tri[^{3}H]oleate ([^{3}H]TO) and [^{14}C]cholesteryl oleate ([^{14}C]CO), were prepared as described previously[8]. Mice were fasted for 4 h and injected (t = 0) intravenously with 200 μL of TRL-like particles (1 mg TG per mouse). Blood samples were taken from the tail vein at 2, 5, 10 and 15 min after injection to determine the plasma decay of [^{3}H]TO and [^{14}C]CO. Plasma volumes were calculated as 0.04706 × body weight (g)[9]. After 15 min, mice were killed by cervical dislocation and perfused with ice-cold PBS. Subsequently, livers were isolated and weighted. One piece of liver was dissolved overnight at 56°C in Tissue Solubilizer (Amersham Biosciences, Roosendaal, The Netherlands), and ^{3}H- and ^{14}C-activity were quantified.

Lipid droplet-positive area quantification

At the end of the third experiment, after 12-weeks of treatment, interscapular brown fat and subcutaneous white adipose tissue (scWAT) were collected. Tissues were fixed in 4% paraformaldehyde, dehydrated in 70% ethanol and embedded in paraffin. Tissue sections (5 μm) were stained with hematoxylin-eosin (HE). The area of intracellular lipid droplets in brown fat and scWAT were quantified using ImageJ software (version 1.50i).

Atherosclerosis quantification

At the end of the third experiment, after 12-weeks of treatment, hearts were collected, fixed in phosphate-buffered 4% formaldehyde, and embedded in paraffin. Samples were cross-sectioned (5 μm) perpendicular to the axis of the aorta throughout the aortic root area, starting from the appearance of open aortic valve leaflets. To evaluate atherosclerosis development, four sections with 50 μm-intervals were used and stained with haematoxylin-phloxine-saffron (HPS) for histological analysis. Lesions were categorized for lesion severity according to the guidelines of the American Heart Association adapted for mice [10] and classified as mild lesions (types 1 - 3) and severe lesions (types 4 - 5). Monoclonal mouse antibody M0851 against smooth muscle cell (SMC) actin was used to quantify the SMC area. Sirius Red staining was used to quantify the collagen area. Rat monoclonal antibody MAC3 was used to quantify macrophage area as described [2]. Lesion area was determined with Image J Software

(version 1.50i).

Supplemental table 1: Primer sequences

Gene	Forward Primer Sequence (5'-3')	Reverse Primer Sequence (5'-3')
36b4	GGACCCGAGAAGACCTCCTT	GCACATCACTCAGAATTTCAATGG
Abcg5	TGTCCTACAGCGTCAGCAACC	GGCCACTCTCGATGTACAAGG
Asbt	CCATGGGGTATCTTCGTGGG	GTTCCCGAGTCAACCCACAT
β2-microglobulin	TGACCGGCTTGTATGCTATC	CAGTGTGAGCCAGGATATAG
Bsep	CTGCCAAGGATGCTAATGCA	CGATGGCTACCCTTTGCTTCT
Cyp7a1	CAGGGAGATGCTCTGTGTTCA	AGGCATACATCCCTTCCGTGA
Cyp7b1	CAGCTATGTTCTGGGCAATG	TCGGATGATGCTGGAGTATG
Cyp8b1	GGACAGCCTATCCTTGGTGA	CGGAACTTCCTGAACAGCTC
Cyp27a1	TCTGGCTACCTGCACTTCCT	CTGGATCTCTGGGCTCTTTG
Fgf15	ACGGGCTGATTCGCTACTC	TGTAGCCTAAACAGTCCATTTCCT
Fxr	GGCCTCTGGGTACCACTACA	ACATCCCCATCTCTTTGCAC
Hsd3b7	CCATCCACAAAGTCAACGTG	CTCCATTGACCTTCCTTCCA
Mrp2	GCTTCCCATGGTGATCTCTTC	ATCATCGCTTCCCAGGTACTG
Ntcp	CTTCACTGCCTTGGGCATGATG	TGTTTCCATGCTGATGGTGCG
Oatp1α1	TGAGAAAGACAGCAGTAG-GACTTT	GTGATTTGGCTAGGTATGCAC
Ost-α	TGGACCCTGGAAGACATA	TAACCACTGATAAGGCTGAG
Ost-β	GACCACAGTGCAGAGAAAGC	ATTCCAAGGAGCCGCATCT
Shp	TCTGCAGGTCGTCCGACTATT	TGTCTTGGCTAGGACATCCA

Abcg5, ATP-binding cassette sub-family G member 5; *Asbt*, apical sodium–bile acid transporter; *Bsep*, bile salt export pump; *Cyp7a1*,cholesterol 7 alpha-hydroxylase; *Cyp7b1*, oxysterol and steroid 7-alpha-hydroxylase; *Cyp8b1*, sterol 12-alpha-hydroxylase; *Cyp27a1*, sterol 27-hydroxylase; *Fgf15*, fibroblast growth factor 15; *Fxr*, farnesoid X receptor; *Hsd3b7*, hydroxy-delta-5-steroid dehydrogenase; *Mrp2*, multidrug resistance protein 2; *Ntcp*, Na+ taurocholate cotransporting polypeptide; *Oatp1α1*, organic anion transporter family member 1α1; *Ost-α*, organic solute transporter α; *Ost-β*, organic solute transporter β; *Shp*, small heterodimer partner.

Supplemental table 2: Relative gene expressions

Gene	-	β	c	c+β
Asbt	1.00 ± 0.07	**1.28 ± 0.10***	1.05 ± 0.10	**1.25 ± 0.08***
Ost-alpha	1.00 ± 0.05	1.09 ± 0.10	0.95 ± 0.05	1.01 ± 0.08
Ost-beta	1.00 ± 0.05	**1.25 ± 0.10***	1.03 ± 0.08	1.04 ± 0.07
Fxr	1.00 ± 0.06	1.12 ± 0.09	0.99 ± 0.05	1.02 ± 0.05
Fgf15	1.00 ± 0.46	**2.66 ± 0.38***	**0.41 ± 0.13**$^{\#\#\#}$	**1.18 ± 0.51**$^{\$}$
Shp	1.00 ± 0.41	**2.85 ± 0.55****	**0.37 ± 0.10***$^{\#\#\#}$	**0.92 ± 0.28**$^{\#\#\$}$

Values are expressed as mean fold change ± SEM. *P<0.05, **P<0.01 vs -; ##P<0.01, ###P<0.001 vs β; $P<0.05 vs c.

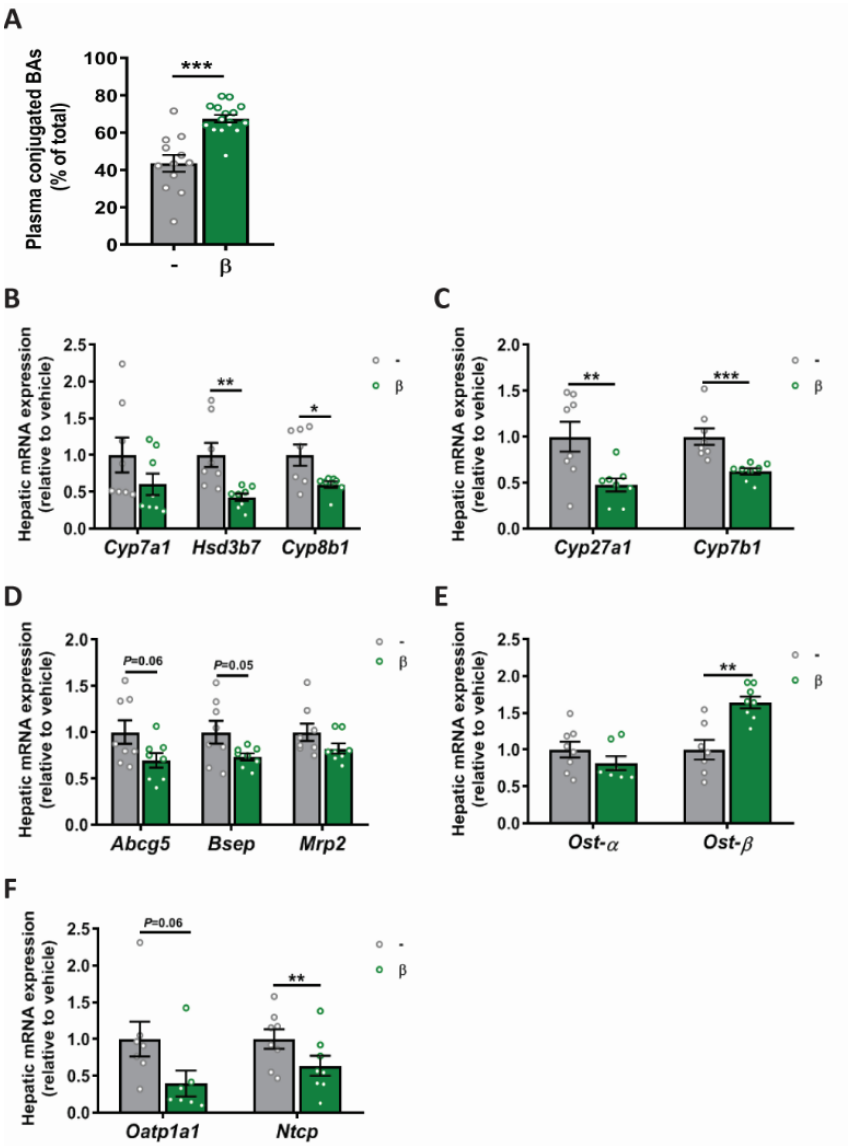

Supplemental Figure 1. Prolonged β3-AR agonism reduces the expression of genes involved in bile acid synthesis. Female *APOE*3-Leiden.CETP* (*E3L.CETP*) mice fed a Western-type diet were treated with the β3-AR agonist CL316,243 (β) or vehicle (-) for 9 weeks. (**A**) Proportion of conjugated BAs in plasma was calculated; n= 14-16 mice/ group. Mice were killed and liver samples were collected to measure mRNA expression of genes involved in (**B**) classical bile acid (BA) synthesis pathway, (**C**) the alternative BA synthesis pathway, (**D**) canalicular BA secretion, (**E**) basolateral BA secretion, and (**F**) basolateral BA uptake. N= 7-8 mice/group. Values are means ± SEM. Differences were determined using the unpaired two-tailed Student's t-test. **P*<0.05, ***P*<0.01, ****P*<0.001 vs vehicle (-).

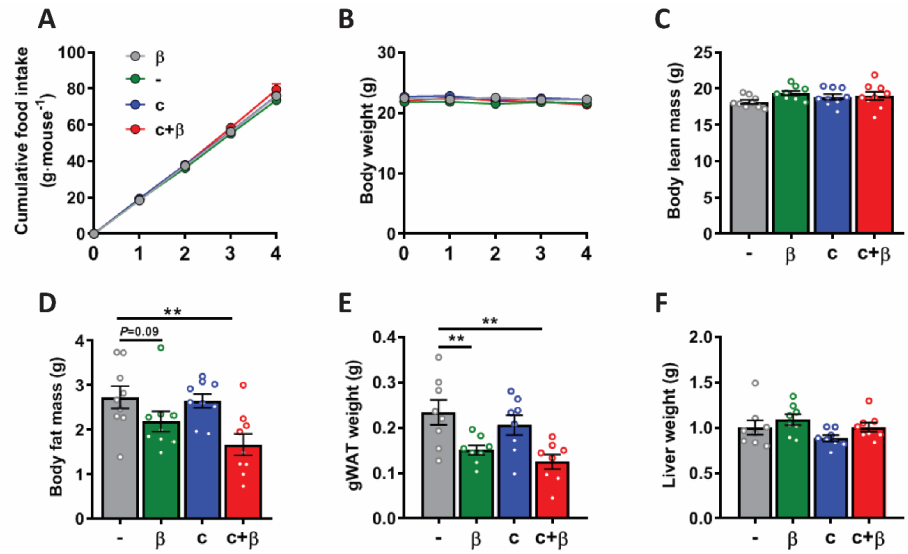

Supplemental Figure 2. Bile acid sequestration does not influence effects of β3-AR agonism on food intake and body composition. *E3L.CETP* mice fed a Western-type diet were treated with vehicle (-), the β3-AR agonist CL316,243 (β), the bile acid sequestrant Colesevelam (c), or their combination (c+β). (**A**) Cumulative food intake and (**B**) body weight were monitored weekly. After 4 weeks, (**C**) body lean mass and (**D**) fat mass were determined. Mice were killed and (**E**) gonadal white adipose tissue (gWAT) and (**F**) liver were weighted. N = 8-9 mice/group. Values are means ± SEM. Differences between four groups were determined using one-way ANOVA with the LSD posthoc test. **P*<0.05, ***P*<0.01 vs vehicle (-).

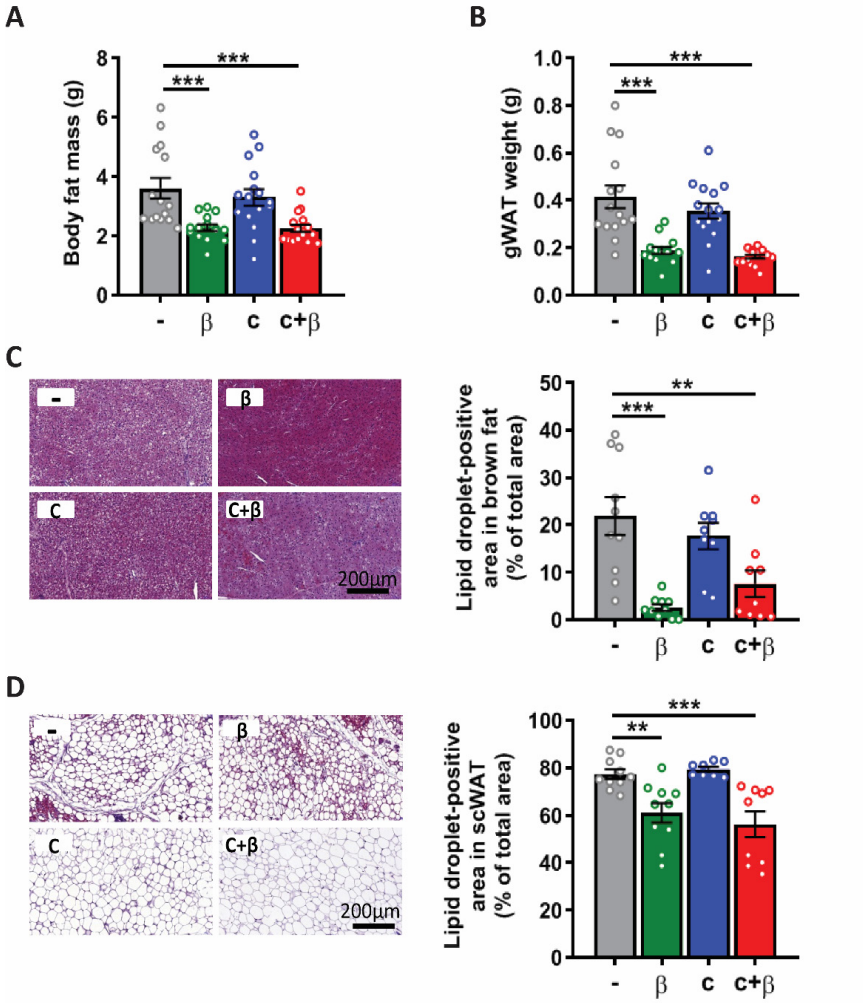

Supplemental Figure 3. Bile acid sequestration on top of β3-AR agonism does not further **influence food intake, body fat mass, brown fat activity, browning of white adipose tissue, and lesion severity.** *E3L.CETP* mice fed a Western-type diet were treated with vehicle (-), the β3-AR agonist CL316,243 (β), the bile acid sequestrant Colesevelam (c), or their combination (c+β). After 12 weeks, (**A**) fat mass was measured. Mice were killed and (**B**) gonadal white adipose tissue (gWAT) were isolated and weighted; n= 14-16 mice/ group. (**C**) Interscapular brown fat and (**D**) subcutaneous white adipose tissue (scWAT) were stained with hematoxylin-eosin (H&E) to quantify lipid droplet-positive area; n= 8-10 mice/ group. Values are means ± SEM. Differences between four groups were determined using one-way ANOVA with the LSD posthoc test. ***P*<0.01, ****P*<0.001 vs vehicle (-).

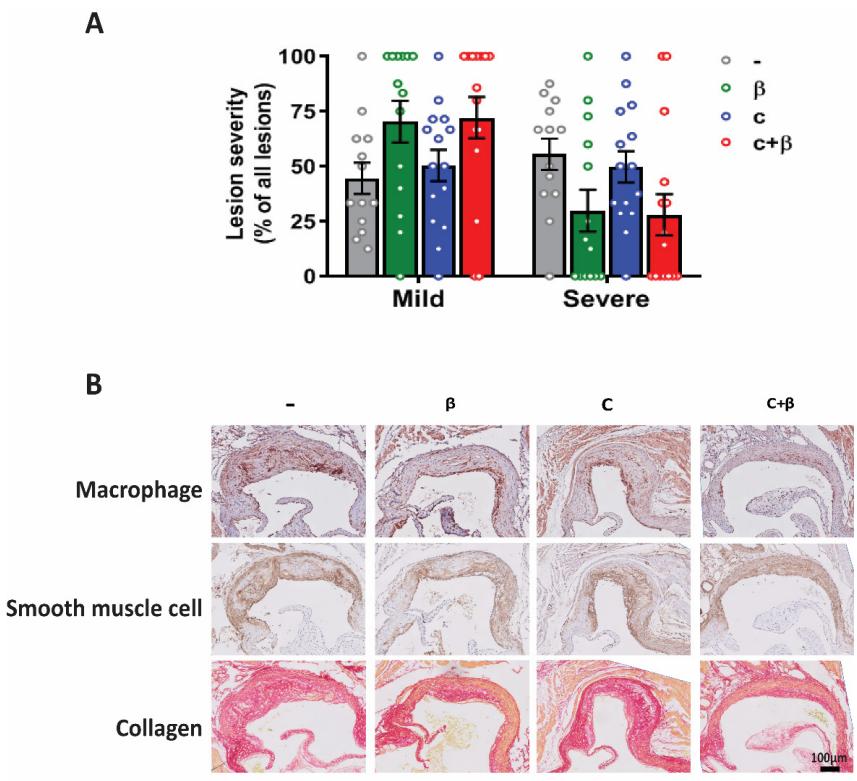

Supplemental Figure 4. Bile acid sequestration on top of β3-AR agonism decreases the percentage of macrophage area within the lesion and increases plaque stability index. *E3L.CETP* mice fed a Western-type diet were treated with vehicle (-), the β3-AR agonist CL316,243 (β), the bile acid sequestrant Colesevelam (c), or their combination (c+β) for 12 weeks. (**A**) Atherosclerotic lesion severity in aortic root area of each group was evaluated. (B) Lesions were characterized by staining of macrophages, smooth muscle cells and collagen. Values are means ± SEM.

Supplemental references

1. Westerterp, M., et al., *Cholesteryl ester transfer protein decreases high-density lipoprotein and severely aggravates atherosclerosis in APOE*3-Leiden mice.* Arterioscler Thromb Vasc Biol, 2006. **26**(11): p. 2552-9.
2. Hoeke, G., et al., *Atorvastatin accelerates clearance of lipoprotein remnants generated by activated brown fat to further reduce hypercholesterolemia and atherosclerosis.* Atherosclerosis, 2017. **267**: p. 116-126.
3. Hulzebos, C.V., et al., *Measurement of parameters of cholic acid kinetics in plasma using a microscale stable isotope dilution technique: application to rodents and humans.* J Lipid Res, 2001. **42**(11): p. 1923-9.
4. Hulzebos, C.V., et al., *Cyclosporin a and enterohepatic circulation of bile salts in rats: decreased cholate synthesis but increased intestinal reabsorption.* J Pharmacol Exp Ther, 2003. **304**(1): p. 356-63.
5. van der Veen, J.N., et al., *Activation of the liver X receptor stimulates trans-intestinal excretion of plasma cholesterol.* J Biol Chem, 2009. **284**(29): p. 19211-9.
6. Eggink, H.M., et al., *Transhepatic bile acid kinetics in pigs and humans.* Clin Nutr, 2018. **37**(4): p. 1406-1414.
7. Bijland, S., et al., *Fenofibrate increases very low density lipoprotein triglyceride production despite reducing plasma triglyceride levels in APOE*3-Leiden.CETP mice.* J Biol Chem, 2010. **285**(33): p. 25168-75.
8. Rensen, P.C., et al., *Selective liver targeting of antivirals by recombinant chylomicrons--a new therapeutic approach to hepatitis B.* Nat Med, 1995. **1**(3): p. 221-5.
9. Jong, M.C., et al., *Apolipoprotein C-III deficiency accelerates triglyceride hydrolysis by lipoprotein lipase in wild-type and apoE knockout mice.* J Lipid Res, 2001. **42**(10): p. 1578-85.
10. Wong, M.C., et al., *Hepatocyte-specific IKKbeta expression aggravates atherosclerosis development in APOE*3-Leiden mice.* Atherosclerosis, 2012. **220**(2): p. 362-8.